New Journal of Physics
An Institute of Physics and Deutsche Physikalische Gesellschaft Journal

Synthesis and magnetic properties of nanoscale bimetallic Co_1Rh_1 particles

D Zitoun[1], C Amiens[1], B Chaudret[1]†, M Respaud[2], M-C Fromen[3], P Lecante[3] and M-J Casanove[3]

[1] Laboratoire de Chimie de Coordination-CNRS, 205 Route de Narbonne, 31077 Toulouse Cedex 04, France
[2] Laboratoire National des Champs Magnétiques Pulsés et Laboratoire de la Physique de la Matière Condensée, INSA, 135 avenue de Rangueil, 31077 Toulouse, France
[3] Centre d'Elaboration des Matériaux et d'Etudes Structurales-CNRS, BP 4347, 29 rue Jeanne Marvig, 31055 Toulouse Cedex, France
E-mail: chaudret@lcc-toulouse.fr

New Journal of Physics **4** (2002) 1.1–1.11 (http://www.njp.org/)
Received 11 July 2002
Published

Abstract. The influence of size reduction on the magnetism of CoRh has been studied on a system of spherical bimetallic nanoparticles embedded in a polymer matrix. By varying the concentration and the nature of the polymer, we achieved the chemical synthesis of different sizes from 1.7 to 4.1 nm from organometallic precursors. Pulsed fields up to 30 T were used in order to approach the magnetic saturation M_S. Particles with a mean diameter of 1.7 nm display a value of 2.38 μ_B per CoRh unit, strongly enhanced compared to values calculated or measured on a bulk alloy. For all samples, the magnetic moment per atom and the effective anisotropy constant are found to decrease with size but are still enhanced compared to bulk values. These results were interpreted as first evidence of the cooperative role of both alloying and size reduction in the enhancement of the magnetization and the anisotropy in this system associating a three-dimensional ferromagnetic metal with a 4d metal.

1. Magnetic clusters of 3d and 4d metals

One of the most active research topics of the past few years is the investigation of finite size effects in magnetic materials [1]. Technological developments require more and more magnetic

† Author to whom any correspondence should be addressed.

nanomaterials of controlled properties taking advantage of their small size. When decreasing the size of magnetic particles, a transition occurs from polydomain to monodomain magnetic systems. When the thermal energy is sufficiently high, a superparamagnetic (SP) behaviour can be observed [2].

The crystallographic structure is also expected to be modified drastically as already mentioned in both experimental and theoretical studies. Another aspect of nanoscale materials is the large number of surface atoms; for a 2 nm cluster, half of the atoms are surface atoms. These trends lead to the modification of the electronic band structure, at the border of the molecular and metallic states, and induce unusual magnetic properties for nanoscale clusters.

1.1. 3d magnetic clusters

As a consequence of surface effects, an enhanced magnetic moment is predicted for clusters of 3d ferromagnetic (FM) metals. Such a phenomenon was first demonstrated in the case of Fe, Co and Ni metal clusters containing fewer than 1000 atoms, using molecular beam deflection measurements in high vacuum [3]. The clusters with fewer than 500 atoms display an enhancement of the magnetic moment per atom from the bulk value up to the atomic value.

1.2. 4d magnetic clusters

Recently, the case of 4d metals has been addressed. Bulk 4d metals do not display any FM behaviour. However, a spin polarization can be induced by a very small perturbation of the lattice parameter, by elaborating layered structures with an FM material [4] and more efficiently by alloying with a 3d FM metal [5]. An element sensitive technique (namely XMCD) was recently used to measure the spin and orbital contributions of rhodium in CoRh [6] and FeRh [7] alloys. Size reduction also induces the appearance of FM as demonstrated by molecular beam deflection measurements for Rh nanoparticles up to 34 atoms [8], in agreement with theoretical calculations based on tight binding methods [9]. Considering these results, size reduction promotes in some cases an electronic polarization in species at the border of FM. Rh is a typical example. As a consequence, one can expect unusual magnetic behaviours in Rh-3d FM bimetallic clusters, where both size reduction and alloying should play an important role in the electronic spin polarization.

In this article, we report the first synthesis and magnetic study of bimetallic CoRh nanomaterials consisting in isolated particles of diameter below 5 nm and their magnetic characterization. Their magnetic data clearly demonstrate the bimetallic nature of the CoRh nanoparticles with reduced exchange energy between the nearest neighbours and larger magnetic anisotropy. The main result concerns the saturation magnetization of this system. Spectacularly, high fields up to 30 T are not sufficient to fully saturate the magnetization of the smaller nanoparticle system which reaches a value twice the predicted bulk value for a CoRh alloy, suggesting a huge influence of the particle size reduction.

2. Chemical synthesis

The chemical synthesis of nanoparticles is very attractive considering how easily one can design and functionalize a specific material [10]. The aim of this work is to study the individual

magnetic properties of nanoparticles [11]. So the synthesis has to lead to assemblies of identical particles with pure surface state and no magnetic interactions.

2.1. The organometallic route

The synthesis of well defined nanoparticles with a diameter size in the range of 1–3 nm is therefore an important challenge. Several routes have been explored, using vapour condensation or electrochemical reduction of salts [12]. Our group has developed an organometallic approach towards the synthesis of metal nanoparticles. A neutral low-valent polyene complex of the desired metal is reacted with a reducing gas in mild conditions of pressure and temperature. In a polymer like poly(vinylpyrrolidone) (PVP), the synthesis leads to well dispersed nanoparticles with narrow size distribution of monometallic Ni [13], Co [14], Ru [15], Rh, Pd and Pt [16]. In the case of cobalt, magnetic measurements can be correlated to the results obtained on clusters from gas phase experiments. The magnetic moment per atom is enhanced up to 1.94 μ_B for clusters of about 150 atoms [17]. The nanoparticles behave like free clusters, which means that the dipolar interactions between particles are negligible, and the interaction with the polymer matrix is apparently too weak to induce any electronic perturbation. High field magnetization and FM resonance were also performed, which definitely confirm the enhancement of both magnetic moment and anisotropy [18]. These systems were structurally characterized via high resolution transmission electron microscopy (HRTEM) and wide angle x-ray scattering (WAXS) evidencing in the case of cobalt an unusual icosahedral structure.

Using the same chemical route, the synthesis of bimetallic nanoparticles has been achieved by simultaneous decomposition of two organometallic precursors in an organic solution of PVP. This procedure has already been successfully applied to the synthesis of Pd_xCu_{1-x} [19] and Pt_xRu_{1-x} [20]. Also, using a similar approach, Co_xPt_{1-x} [21] bimetallic isolated magnetic particles of nanometric size and adjustable composition have been obtained. They allow us to demonstrate the influence of the Pt concentration on the anisotropy.

2.2. Synthesis of nanoscale CoRh particles

Three systems of well isolated CoRh particles with sizes near 1.7, 2.6 and 4.1 nm, namely Coll.1, Coll.2 and Coll.3, embedded in an organic polymer, have been synthesized using the organometallic approach mentioned above.

The first two samples consist of particles dispersed in PVP; the third one consists of particles dispersed in poly(2, 6-dimethyl phenylene oxide) (PPO). The particles (Coll.1 and Coll.2) are synthesized by the simultaneous decomposition of two organometallic precursors $Co(\eta^3\text{-}C_8H_{13})(\eta^4\text{-}C_8H_{12})$ and Rh(acetylacetonate)$(\eta^4\text{-}C_8H_{12})$ in a tetrahydrofuran (THF) solution containing PVP. The initial homogeneous solution is submitted to a dihydrogen pressure of 3 bars. The reduction of the olefins and the metals is complete after 20 h vigorous mixing at room temperature. A precipitate is first obtained by cooling the solution down to $-80\,^{\circ}$C. Further colloid precipitation is obtained upon addition of methanol and pentane. Samples Coll.1 and Coll.2 are obtained as black powders after filtration and drying under vacuum. The particle size is increased by varying the overall initial concentration of metal precursors in polymer from 10 to 20 wt%. The initial atomic cobalt/rhodium ratio is equal to one. The final atomic composition of the samples is determined by chemical microanalysis. This procedure leads to two bimetallic systems (Coll.1 and Coll.2) of respective composition

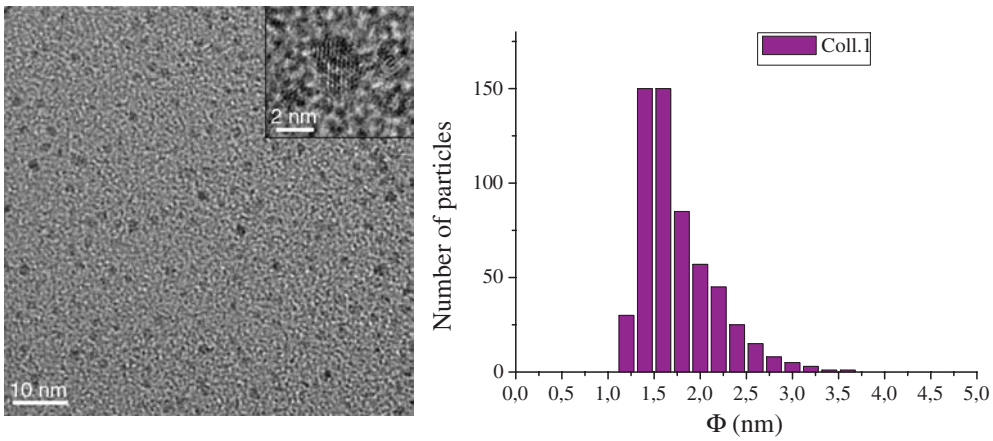

Figure 1. (a) TEM image of Coll.1. Inset of an HREM micrograph of one particle. (b) Size histogram of a collection of 600 particles.

$Co_{0.47}Rh_{0.53}$ and $Co_{0.55}Rh_{0.45}$, for an initial ratio metal/polymer of 10 and 20 wt%. The final metal/polymer ratios are respectively 8.7 and 15.8 wt%.

By changing the polymer/solvent couple, one can also change the diffusion rate of the atoms and clusters in solution and thus further change the size. When using PPO in anisole and an overall initial concentration of metal precursors in polymer of 10 wt%, Coll.3 is obtained as black pellets. The microanalysis gives an atomic composition of $Co_{0.50}Rh_{0.50}$ and a final metal content of 5.07 wt%.

3. Characterization of the colloids

3.1. Transmission electron microscopy

Figure 1(a) shows a low magnification transmission electron microscopy (TEM) image of Coll.1 showing nanoparticles homogeneous in size with a mean diameter of $\Phi = 1.7(\pm 0.4)$ nm (Coll.1)‡. Increasing the initial metal precursor content (20 wt%) leads to slightly bigger particles of $\Phi = 2.6(\pm 0.7)$ nm (Coll.2). Both systems consist of isolated nanoparticles displaying a narrow size distribution (figure 1(b)). When observed in high resolution mode, neither Coll.1 nor Coll.2 display a well defined crystalline order (see inset of figure 1 for Coll.1). The lattice fringes spaced by 0.22 nm observed in some particles do not provide enough elements to decide in favour of a particular phase.

The particles in PPO form some aggregates of about ten particles with a particle mean diameter $\Phi = 4.1(\pm 0.6)$ nm (figure 2). When observed in high resolution, Coll.3 displays a well defined crystalline order, some particles display a hexagonal close packed (HCP) structure while some display a face centred cubic (FCC) structure. In both cases, the lattice parameters correspond to a CoRh alloy. It is noteworthy that for bulk materials the transition from FCC to HCP structure occurs for a cobalt ratio of 0.495, very close to the cobalt content in Coll.3.

‡ The particle size is determined by the software Optimas on an assembly of more than 500 particles.

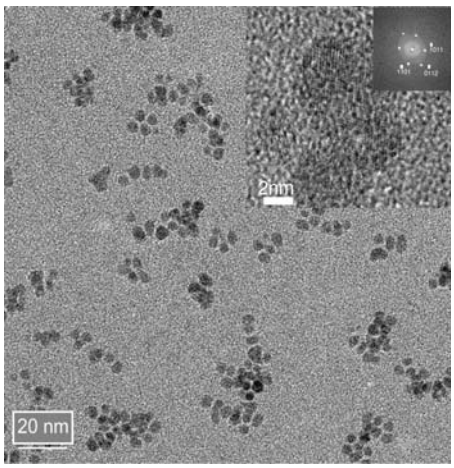

Figure 2. HREM micrograph of Coll.3. Inset: HCP particle with the Fourier transform of the image.

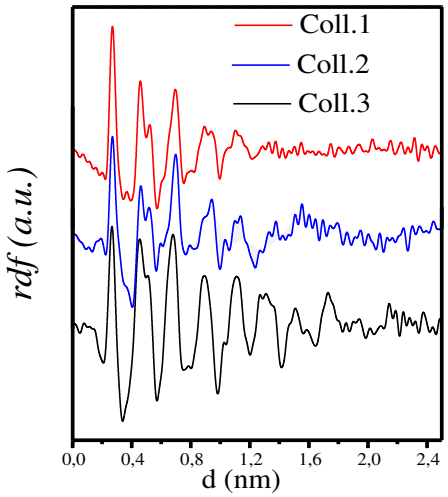

Figure 3. RDF of the three samples.

3.2. X-ray scattering

WAXS was performed on the three samples. The radial distribution functions (RDFs) obtained display a broad pattern, which does not correspond to the conventional periodic crystalline phases. The coherence lengths close to 1.4 nm (1.8 and 2.1 nm) for Coll.1 (figure 3) (Coll.2 and Coll.3) are smaller than the mean diameters observed by TEM. This shortening may be related to a disordered surface and for Coll.3 to the polycrystallinity of the particles. For the three colloids, the first peak in the RDF is sharp enough to exclude significant distance dispersion and clearly indicates the metallic (i.e. non-oxidized) character of the particles. The first metal–metal distances d_{MM} are found to be 0.269 nm for Coll.1 and Coll.2 and 0.266 nm for Coll.3, larger than those found in bulk CoRh alloys (cubic parameter: 0.262 ± 0.001 nm). The colloids display a d_{MM} very close to that of bulk rhodium (cubic parameter: 0.269 nm) [22]. The RDFs obtained for Coll.1 and Coll.2 do not correspond to the crystalline phases of the bulk materials.

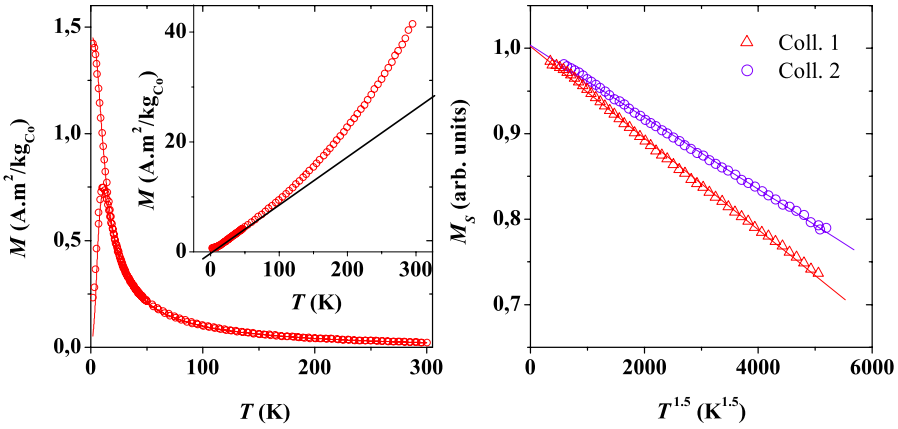

Figure 4. (a) ZFC/FC magnetization of Coll.1 (○) and the best fit (—) obtained for 1.65 nm nanoparticles with a lognormal distribution of size and a size dispersion of 0.14 with an anisotropy value of 1.0×10^6 J m^{-3}. The inset shows the departure from the Curie law (—). (b) Variation of the normalized M_S versus $T^{3/2}$ for Coll.1 and Coll.2 which are following Bloch laws.

Furthermore, the atomic arrangement in the particles seems very similar to the non-periodic one observed for other systems of nanoparticles (Co [23], Rh [24], CoPt [21]).

For Coll.3, the pattern is almost the same but the peaks are a little broader. The RDF may result from an assembly of FCC and HCP particles with a polycrystalline structure as evidenced by HREM experiments.

4. Magnetic properties

The magnetic properties have been investigated in steady field up to 5 T with a commercial SQUID magnetometer (MPMS Quantum Design). The high field magnetization measurements up to 30 T have been performed using long pulsed fields [25]. In the following, for convenience, the magnetization data have been normalized according to the Co contents although the magnetic moment is also carried by the Rh atoms in the bulk phase. Therefore, in a first step we have considered that all the magnetization is localized on the Co site. This value also corresponds to the magnetization per CoRh unit.

Figure 4(a) shows a typical zero-field-cooled–field-cooled (ZFC–FC) magnetization versus temperature (T) curve measured in a low magnetic field of 1 mT for the smallest particles (Coll.1). It evidences a typical SP behaviour with a blocking temperature $T_B = 10.9$ K. The inverse of the magnetization versus T shown in the inset of figure 2(a) does not follow the classical Curie law. Coll.2 displays the same behaviour with $T_B = 13.5$ K. Coll.3 also displays a SP behaviour for temperature above the blocking temperature ($T_B = 38$ K) (figure 5). The curves have been fitted using a method described in a previous article [26]; the parameters of the fit are listed in table 1.

The evolution with the size of particles of the hysteresis loops measured at 2 K (figure 6) displays several interesting trends. First, a huge enhancement of the magnetization determined at $\mu_0 H = 5$ T is depicted around 1.9 μ_B per CoRh unit, independently of the mean size. The square shape of the loop increases with size and the magnetic susceptibility at high field

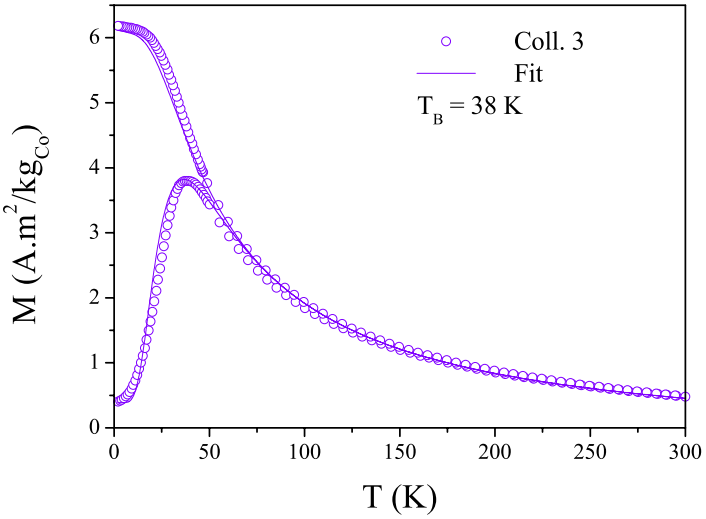

Figure 5. (○) ZFC/FC curve of Coll.3 (CoRh in PPO). The best fit was obtained for 4.9 nm nanoparticles with a lognormal distribution of size and a size dispersion of 0.13; the anisotropy is 0.12×10^6 J m^{-3}.

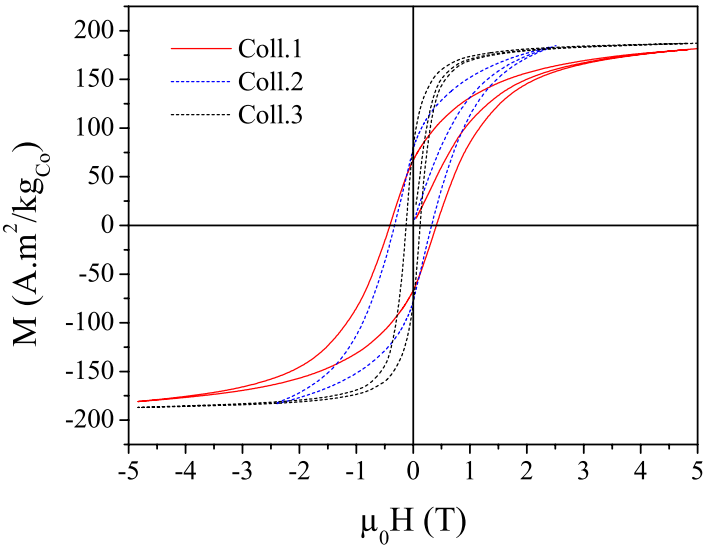

Figure 6. Hysteresis loops for the three samples in steady fields at 2 K.

Table 1. Parameters of the three colloidal samples.

Sample	Composition	ϕ^{a} (nm)	ϕ^{b} (nm)	σ^b	T_B^{b} (K)	K_{eff}^{b} (10^6 J m^{-3})	μ_{CoRh} (5 T) (μ_B)	α (K$^{1.5}$)
Coll.1	$Co_{47}Rh_{53}$	1.7	1.65	0.14	10.9	1.0	1.91	5.32×10^{-5}
Coll.2	$Co_{55}Rh_{45}$	2.6	2.3	0.15	13.5	0.6	1.88	4.5×10^{-5}
Coll.3	$Co_{50}Rh_{50}$	4.1	4.9	0.13	38	0.12	1.93	

[a] Deduced from the HRTEM micrographs.
[b] Deduced from the ZFC/FC magnetization curves.

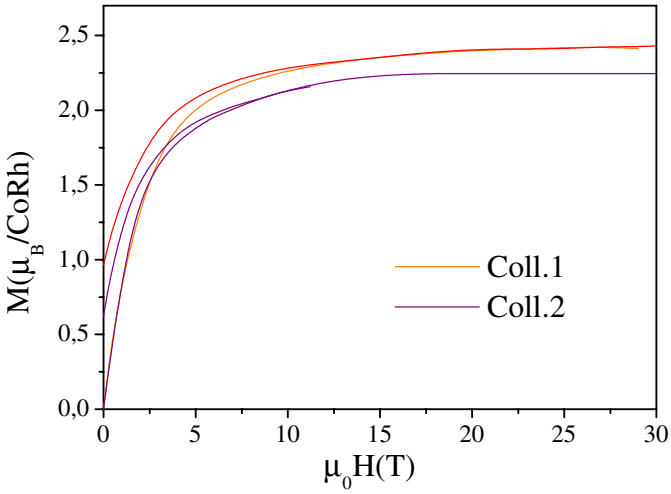

Figure 7. Pulsed high field magnetization curves up to 35 T at $T = 4.2$ K.

Table 2. Magnetic data at high field.

Sample	$\mu_0 H_{C(T=0\ \mathrm{K})}$ (T)	μ_{CoRh} (32 T) (μ_B)	$\mu_0 H_{\mathrm{irreversibility}}$ (T)
Coll.1	0.99	2.38	13
Coll.2	0.60	2.30	8.2
Coll.3	0.15	1.93[a]	3.2

[a] The magnetization is saturated at 5 T.

decreases with size. At the same time, the coercive field also decreases. This is a clear evidence of the enhancement of the anisotropy field with reducing size [27], and thus of the anisotropy as previously observed in 3d magnetic clusters [28]. In our case, no clear explanation can be proposed since this effect may result from a change in surface anisotropy and/or from a specific magnetocrystalline anisotropy resulting from the unusual crystallographic structure (Coll.1, Coll.2).

In order to get more information about the saturation magnetization, pulsed high field magnetization measurements were undertaken (table 2). Figure 7 shows the first magnetization and remanence curves of both colloids up to 30 T at 4.2 K. A magnetic saturation was obtained for Coll.2 in fields above 15 T, while a vanishing differential susceptibility persists for Coll.1 even in high fields. Unusual irreversibility phenomena are occurring in high fields up to $H_{irr} = 13$ T (8.2 T) for Coll.1 (Coll.2) up to four times larger than for Coll.3 (3.2 T). Their magnitude remains constant even when changing the magnetic field sweeping rate, allowing us to discard possible dynamic effects. We interpret the difficulty of reaching the magnetic saturation as possible evidence of surface canting.

At 30 T, the average magnetic moments per CoRh unit are 2.38 and 2.3 μ_B for Coll.1 and Coll.2. For monometallic Co particles using the same experimental set-up, the moment was found to be 2.1 and 1.9 μ_B per Co atom for particles with an average number of atoms of 150 and 300 respectively. More spectacularly, these values are twice the predicted bulk value for a CoRh alloy (theoretical value: 1.17 μ_B per CoRh unit) [29].

5. Discussion

This set of magnetic data opens new questions concerning the influence of the size on the magnetism of this 3d–4d FM bimetallic compound. These unusual magnetic properties should be interpreted in connection with both the nanometric size of the particles and the possible organization and distribution of the two elements (Co, Rh) in a particle.

Concerning Coll.3, the structure is clear enough. The HRTEM study seems to be consistent with an FCC/HCP mixture of nanoparticles. Some particles are monocrystalline and some polycrystalline which may explain the small coherence length observed by WAXS compared to the diameter determined by TEM. The atomic distribution is thus homogeneous in the particle. Since both the crystalline phase and the lattice parameters correspond to bulk CoRh, Coll.3 is structurally determined as an alloy.

For the systems of smaller size, Coll.1 and Coll.2, since the atomic organization is not identified, three hypotheses can be made. The first one consists in CoRh alloyed particles with a non-periodic crystalline structure. The other ones are based on segregated particles with a core–shell structure, namely Co at the core and Rh in the outer shell and vice versa. Let us first discuss these segregated models. Considering M_S both hypotheses can be possible: Co should possess a high magnetic moment due to the small size of the core or to the small thickness of the outer shell, and an induced spin polarization on the Rh sites in contact with Co can be predicted as in the case of multilayer systems. However, the first hypothesis of a Co core can be easily rejected, since it would lead to very small size compared to the coherence length of the systems. Moreover, in segregated nanoparticles, the surface sites should be occupied by the element with the lower surface energy, namely the Co in this case [30]. Furthermore, the values of d_{MM} deduced from the WAXS studies are larger than the expected values for the CoRh alloy and close to those of Rh. Thus, the hypothesis of segregation favours the occurrence of a Rh rich core surrounded by a Co shell. In that context, most of the magnetization should be carried by the outer surface atoms [31]. This will lead to a faster decrease of the saturation magnetization upon warming in contradiction with our experimental results. The magnetic data of Coll.1 and Coll.2 are in agreement with an alloyed structure. The three systems display a clear evolution of the magnetic properties with particle size (magnetization saturation, anisotropy, hysteretic field and irreversibility field) and Coll.3 is structurally determined as an alloy.

If one assumes that the bulk ratio $\mu_{\mathrm{Rh}}/\mu_{\mathrm{Co}}$ theoretically determined by Moraïtis *et al* [30] is still valid at these sizes, the magnetic moments on each metal are estimated to be $\mu_{\mathrm{Co}} = 2.02\ \mu_B$ and $\mu_{\mathrm{Rh}} = 0.32\ \mu_B$ for Coll.1. For bulk CoRh of the same composition, the calculated magnetic moments are $\mu_{\mathrm{Co}} = 1.01\ \mu_B$ and $\mu_{\mathrm{Rh}} = 0.16\ \mu_B$; the magnetic properties are thus strongly enhanced as a result of size reduction. The smaller system, Coll.1, has the lower Co content but displays the higher M_S. This can be qualitatively explained considering that the reduced Co concentration is overcompensated by size reduction. The size effect is still important up to 4.1 nm, and applying the same hypothesis, the magnetic moments for Coll.3 can be estimated at $\mu_{\mathrm{Co}} = 1.64\ \mu_B$ and $\mu_{\mathrm{Rh}} = 0.29\ \mu_B$. The magnetic moment on the Co site can be compared to the one in monometallic cobalt particles; for the same particle size, the magnetic moment reaches almost the same value [26, 32].

6. Conclusion

In conclusion, we report in this article the first preparation of cobalt/rhodium nanoparticles by an organometallic route. The bimetallic, most probably alloyed, character of the particles was demonstrated by both structural and magnetic studies which reveal the influence of size reduction. The anisotropy is enhanced by size reduction. We observe an enhancement of the magnetization, up to twice the value of the bulk alloy for the 1.7 nm particles. The main conclusion is that the size reduction and the association with a 3d FM compound play a cooperative role that leads to a probable enhanced induced electronic spin polarization on the Rh atoms, and preserve the Co magnetism. Some XMCD (x-ray magnetic circular dichroism) measurements have been performed to measure the spin and orbital magnetic moment on Rh and will be the subject of a further article.

References

[1] de Jongh L J (ed) 1994 *Physics and Chemistry of Metal Cluster Compounds* (Kluwer: Academic)
Meiwes-Broer K-H (ed) 2000 *Metal Clusters at Surfaces* (Berlin: Springer)
[2] Néel L 1949 *Ann. Geophys.* **99** 5
[3] Billas I M L, Châtelain A and de Heer W A 1994 *Science* **265** 1662
[4] Dinia A, Zoll S, Gester M, Stoeffler D, Jay J P, Ounadjela K, van den Berg H A M and Rakoto H 1998 *Eur. Phys. J.* B **5** 203
[5] Fallot M 1938 *Ann. Phys., Paris* **10** 291
Von W Köster and Horn E 1952 *Z. Metall.* **43** 444
[6] Harp G R, Parkin S S P, O'Brien W L and Tonner B P 1995 *Phys. Rev.* B **51** 12 037
[7] Chaboy J, Bartolomé F, Ibarra M R, Marquina C I, Algabarel P A, Rogalev A and Neummann C 1999 *Phys. Rev.* B **59** 3306
[8] Cox A J, Louderback J G, Apsel S E and Bloomfield L A 1994 *Phys. Rev.* B **49** 12 295
[9] Villaseñor-Gonzalez P V, Dorantes-Davila J, Dreyssé H and Pastor G M 1997 *Phys. Rev.* B **55** 15 084
[10] Schmid G (ed) 1994 *Clusters and Colloids. From Theory to Applications* (Wienheim: VCH)
[11] Jamet M, Wernsdorfer W, Thirion C, Mailly D, Dupuis V, Melinon P and Perez A 2001 *Phys. Rev. Lett.* **86** 4676
[12] Bönneman H, Braun G, Brijoux W, Bunjmann R, Schulze Tilling A, Seegovel K and Siepen K 1996 *J. Organomet. Chem.* **520** 143
[13] Ould Ely T, Amiens C, Chaudret B, Snoeck E, Verelst M, Respaud M and Broto J-M 1999 *Chem. Mater.* **11** 526–9
[14] Osuna J, de Caro D, Amiens C, Chaudret B, Snoeck E, Respaud M, Broto J-M and Fert A 1996 *J. Phys. Chem.* **100** 14 571
[15] Pan C, Pelzer K, Philippot K, Chaudret B, Dassenoy F, Lecante P and Casanove M J 2001 *J. Am. Chem. Soc.* **123** 7584
[16] Dassenoy F, Philippot K, Ould Ely T, Amiens C, Lecante P, Snoeck E, Mosset A, Casanove M-J and Chaudret B 1998 *New J. Chem.* **22** 703–11
[17] Osuna J, de Caro D, Amiens C, Chaudret B, Snoeck E, Respaud M, Broto J-M and Fert A 1996 *J. Phys. Chem.* **100** 1457
[18] Respaud M, Goiran M, Broto J M, Yang F H, Ould Ely T, Amiens C and Chaudret B 1999 *Phys. Rev.* B **59** 1
[19] Bradley J S, Hill E W, Klein C, Chaudret B and Duteil A 1993 *Chem. Mater.* **5** 254
[20] Pan C, Dassenoy F, Casanove M J, Philippot K, Amiens C, Lecante P, Mosset A and Chaudret B 1999 *J. Phys. Chem.* B **103** 10 098

[21] Ould Ely T, Amiens C, Chaudret B, Dassenoy F, Casanove M-J, Lecante P, Mosset A, Respaud M and Broto J M 2000 *J. Phys. Chem.* B **112** 8137
[22] Köster V W and Horn E 1952 *Z. Metall.* **43** 444
[23] Dassenoy F, Casanove M-J, Lecante P, Snoeck E, Mosset A, Ould Ely T, Amiens C and Chaudret B 2000 *J. Chem. Phys.* **112** 8137
[24] Choukroun R, De Caro D, Chaudret B, Lecante P and Snoeck E 2001 *New J. Chem.* **25** 525
[25] Respaud M, Broto J M, Rakoto H, Fert A, Verelst M, Snoeck E, Lecante P, Mosset A, Thomas L, Barbara B, Osuna J, Ould Ely T, Amiens C and Chaudret B 1998 *Phys. Rev.* B **57** 1
[26] Zitoun D, Respaud M, Fromen M C, Casanove M J, Lecante P, Amiens C and Chaudret B 2002 *Phys. Rev. Lett.* **89** 037203
[27] Respaud M 1999 *J. Appl. Phys.* **86** 556
[28] Wernsdorfer W 2001 *Adv. Chem. Phys.* **118** 99
[29] Moraïtis G, Dreyssé H and Khan M A 1996 *Phys. Rev.* B **54** 7140
[30] Mezey L Z *et al* 1982 *Japan. J. Appl. Rev.* **21** 1569
[31] Lindgard P A and Hendriksen P V 1994 *Phys. Rev.* B **49** 12291
[32] Respaud M 1997 *Thèse* de l'Institut National des Sciences Appliquées de Toulouse